Origin of trapping in multicrystalline silicon

Paul Gundel,[a] Martin C. Schubert, and Wilhelm Warta
Fraunhofer Institute for Solar Energy Systems (ISE), Heidenhofstr. 2, 79110 Freiburg, Germany

(Received 29 April 2008; accepted 11 August 2008; published online 3 October 2008)

Defect sites in silicon, which temporarily capture excess charge carriers (traps), are a promising source of information on defect structures relevant for photovoltaic application of the material. In this work the correlation between traps in *p*-type silicon, structural crystal defects, and impurities is explored in order to find the origin of these traps in multicrystalline silicon. The trap density is compared to the density of different impurities and structural crystal defects. These comparisons reveal that the trap density is positively correlated with the oxygen density and negatively correlated with the density of the metallic impurities analyzed. In addition we show that structural crystal defects are necessary but not sufficient for the existence of high trap densities. In summary, structural crystal defects that are decorated by oxygen precipitates arise as likely origin of trap centers. © *2008 American Institute of Physics*. [DOI: 10.1063/1.2990053]

I. INTRODUCTION

An anomalous increase in the apparent excess carrier lifetime due to trapping of minority carriers under low injection conditions has been reported in many publications. This effect is generally assumed to be caused by trapping of minority carriers,[1,2] a concept that is supported by both injection and temperature dependent measurements.[3,4] In 1953 Fan[5] and in 1955 Hornbeck and Haynes[6] independently developed a theoretical model to describe this trapping of minority carriers. According to recent publications this effect is correlated with dislocations,[1,3,7] but the origin of trap centers in multicrystalline silicon is still unclear, whereas in Czochralski (Cz) silicon oxygen was related to the trapping effect.[8] In this paper the spatially resolved trap density is determined by injection dependent carrier density imaging/infrared lifetime mapping (CDI/ILM) measurements.[7,3] From these measurements the trap density can be extracted by fitting the Hornbeck–Haynes[6] model to the experimental data.[3,7,9] First the spatially resolved trap density is compared to the structural crystal defect density, which shows that structural crystal defects are necessary but not sufficient in order to create high trap densities. The second goal is to determine the further requirements, which need to be fulfilled for the existence of high trap densities. For this purpose the trap density is compared to different metallic impurity densities, and the effect of two different annealing steps on the trap density in Cz silicon is examined. First the effect of the passivation of the Cz-specific defect on the trap density is investigated in detail. Second the effect of an annealing step at 800 °C is studied. In order to find the impact of oxygen on the trap density in multicrystalline silicon, the trap density of an as-cut multicrystalline wafer, which is vertically cut out of an ingot, is measured and compared to the diffusion length of the solar cell that is processed from this wafer. All samples in this paper are *p*-type boron doped and have no surface passivation (unless otherwise noted), in order to avoid a possible distortion of the results by a depletion region at the surface due to a nonoptimal passivation layer. This may cause depletion region modulation (DRM) under injection, an effect that can be mistaken for an increased trapping influence. In Refs. 7 and 10 it was shown that a good surface passivation or an unpassivated surface has no major influence on the trap density.

II. EXPERIMENTAL

A. Trap density imaging

Free minority carriers can be trapped in shallow trap levels or levels with asymmetric capture cross sections for holes and electrons.[6,5] Charge neutrality requires that the trapped minority carriers are compensated by additional majority carriers in steady-state condition. Lifetime measurements such as CDI/ILM are based on the assumption that the excess majority carrier density equals the excess minority carrier density. This assumption does not hold anymore for low injection if trapping occurs. Since CDI/ILM detects the absorption and emission of both majority and minority carriers, CDI/ILM measures a higher apparent lifetime than the actual recombination lifetime in low level injection. Trapping leads to an increasing apparent lifetime with decreasing injection density. The injection dependence of the apparent lifetime τ_{app} following the Hornbeck–Haynes[6] model for *p*-type silicon is[7]

$$\tau_{\mathrm{app}}(\Delta n) = \frac{1}{\alpha_n + \alpha_p}\tau_{\mathrm{rec}}\left[\alpha_n + \alpha_p\left(1 + \frac{n_T(\Delta n)}{\Delta n}\right)\right], \qquad (1)$$

with α_n and α_p as the free carrier absorption coefficients for electrons and holes, respectively, τ_{rec} is the recombination lifetime which is assumed to be injection independent in low injection, Δn is the excess minority carrier density, and n_T is the density of trapped minority carriers, which depends on the trap density N_T and the trap escape ratio r_{esc},[1]

[a]Electronic mail: paul.gundel@ise.fraunhofer.de.

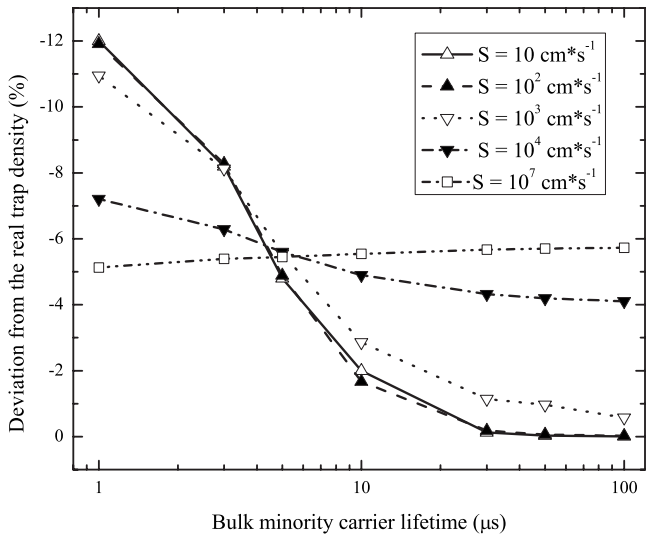

FIG. 1. Simulated deviation of the measured trap density from the actual trap density at different surface recombination velocities in relation to the bulk minority carrier lifetime. The deviation is highest for small lifetimes and ranges up to 12% for the chosen parameters. The thickness of the wafer is 300 μm and the generation parameters of our CDI/ILM setup are used.

$$n_T = \frac{N_T \Delta n}{\Delta n + N_T r_{\mathrm{esc}}}. \tag{2}$$

By fitting this model to a low injection CDI measurement at each point of a wafer, a trap density image can be deduced.[9,7] A qualitative image of the trap density can be obtained by a single CDI/ILM measurement at very low injection.[10]

The trap density is determined by fitting the Hornbeck–Haynes[6] model to the experimental data under the assumption that the injection level in the sample is independent of the depth below the sample surface. Since the assumption is in particular not true in the case of high surface recombination velocities S, we scrutinized how this assumption is influencing our results. For this we simulated the measured apparent lifetimes with injection profiles which were calculated using the continuity equation. From these simulated apparent lifetimes we calculated the trap density with the assumption that the injection level is depth independent. The thickness of the wafer in this simulation is 300 μm, the real bulk minority carrier lifetime was varied in the range from 1 to 100 μs, and the surface recombination velocity from 10 cm s^{-1}, which represents a well passivated surface, to 10^7 cm s^{-1}, which represents an unpassivated as-cut surface. The relative deviation of the measured trap density from the real trap density is independent of the absolute value of the real trap density. The results, which are presented in Fig. 1, show that the measured trap density for the chosen parameters is up to 12% smaller than the actual trap density. Even though this deviation is noticeable, it does not alter the significance of our further results since only wafers with the same surface conditions and similar bulk lifetimes are compared.

For the determination of the trap densities in our experiments, the generation rate was varied between 1.98×10^{14} and 2.21×10^{17} $\mathrm{cm^{-2}\ s^{-1}}$, which leads to an injection level in our samples between approximately 2×10^{10} and 5×10^{13} $\mathrm{cm^{-3}}$. Since these injection levels are very small compared to the doping concentrations of 3.5×10^{15}–1.5×10^{16} $\mathrm{cm^{-3}}$, the effective recombination lifetime can be assumed to be injection independent with sufficient accuracy.

B. Imaging of structural crystal defects

To measure the spatially resolved structural crystal defect density of a large wafer area (up to 156×156 $\mathrm{mm^2}$) qualitatively, the polished wafer is etched in a Secco etch for about 5 min. The Secco etch preferentially attacks the wafer surface where structural crystal defects are present, leading to local etch pits. Since rough surfaces result in a significantly higher emissivity in the infrared range than flat surfaces,[11] a qualitative image of the structural crystal defect density can be obtained by taking a picture of the etched wafer with an infrared camera. Areas with high structural crystal defect densities appear bright, and areas with low structural crystal defect densities appear dark, if the wafer temperature is higher than the background temperature.

III. RESULTS

A. Correlation of traps with structural crystal defects

The qualitative trap density distributions of two cut-outs from different as-cut wafers are compared with the structural crystal defect densities. The qualitative trap density was quantitatively confirmed by fitting the Hornbeck–Haynes[6] model to injection dependent measurements with lower spatial resolution. One of the wafers originates from the top region of a standard multicrystalline ingot, while the other one is from the bottom region of the same ingot. The thickness of both wafers is 270 ± 5 μm, and the doping concentration is about 9.9×10^{15} $\mathrm{cm^{-3}}$.

The structural crystal defect density and the trap density show a high positive correlation in the wafer from the bottom of the ingot (Figs. 2 and 3), which is in good agreement with Refs. 1, 7, and 3. In the wafer of the top region there is a positive correlation in some areas, but there are also regions with high structural crystal defect densities and simultaneously low trap densities (Figs. 4 and 5). Since the trap density of the wafer from the bottom is about one order of magnitude higher than the trap density of the wafer from the top, Figs. 2 and 4 have different color scales. We conclude that structural crystal defects are required for the existence of high trap densities in this sample, but additional conditions such as specific impurity decorations must be fulfilled. The suggestion that structural crystal defects do not necessarily lead to high trap densities was confirmed by an injection dependent CDI/ILM measurement of a 3.5×10^{15} $\mathrm{cm^{-3}}$ gallium doped multicrystalline wafer with float zone purity, which showed an extremely low trap density of less than 2×10^{11} $\mathrm{cm^{-3}}$. The surface of this wafer is polished and unpassivated; the wafer thickness is 660 ± 5 μm. More details on the sample can be found in Ref. 12. In Ref. 8 it was shown that boron doping and gallium doping lead to similar trap densities. In the following the influence of impurities on the trap density is explored.

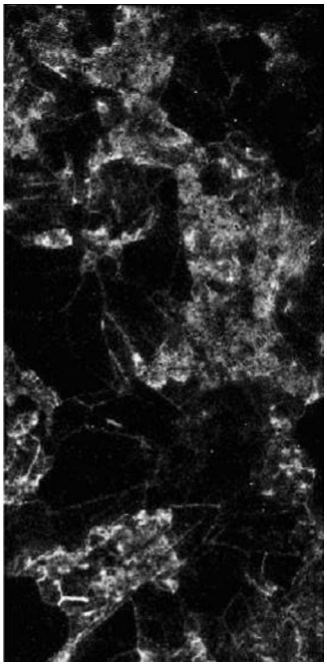

FIG. 2. Qualitative trap density of the wafer from the bottom of the ingot. High trap densities are bright.

B. Influence of impurities

The trap densities of intentionally contaminated and SiN passivated monocrystalline float zone wafers, with a thickness of 390 ± 15 μm and a doping concentration of 1.5×10^{16} cm^{-3}, are determined and compared to the impurity concentrations. The contamination was done in the melt and the impurity concentrations were measured with neutron activation analysis.[13] The wafers probably have an unusual high crystal defect concentration due to their small diameter,

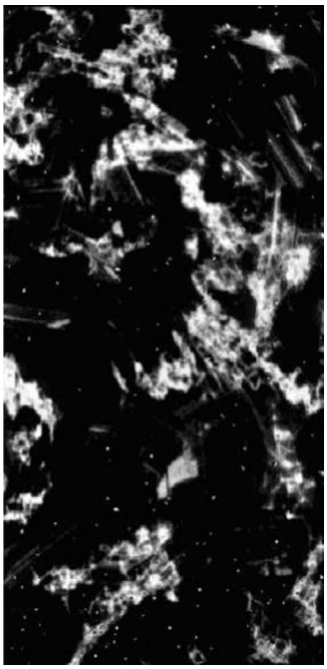

FIG. 3. Qualitative structural crystal defect density of the same area that is depicted in Fig. 1. High structural crystal defect densities are bright. The image shows a high positive correlation with the trap density.

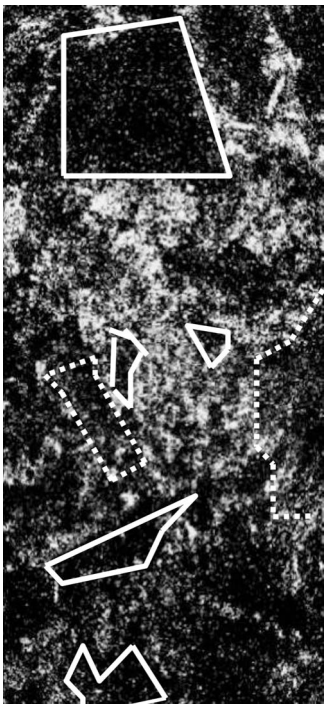

FIG. 4. Qualitative trap density of the wafer from the top of the ingot. High trap densities are bright.

which led to a high cooling rate; more details on the samples can be found in Ref. 13. The high defect concentration can be deduced from the low minority carrier lifetime (smaller than 10 μs) of a reference sample that was not contami-

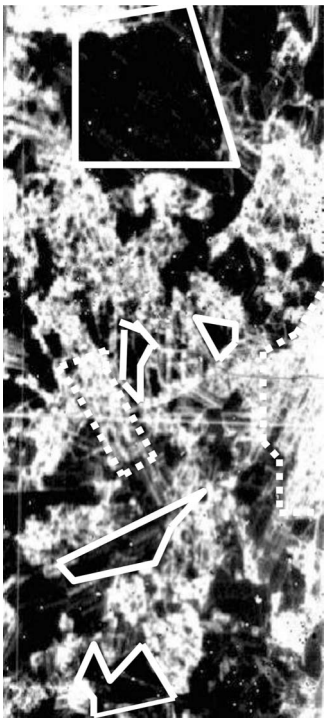

FIG. 5. Qualitative structural crystal defect density of the same area that is depicted in Fig. 3. High structural crystal defect densities are bright. In some areas (i.e., the solid marked areas) there is a positive correlation between trap density and structural crystal defect density, but there are also areas with high structural crystal defect densities and low trap densities (i.e., dashed marked areas).

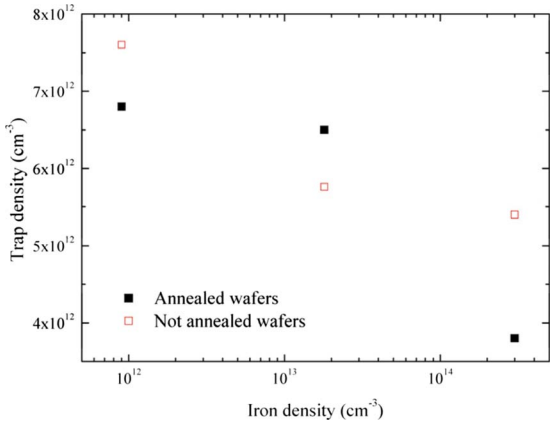

FIG. 6. (Color online) Trap density plotted against iron density. The trap density shows the tendency to be reduced by iron.

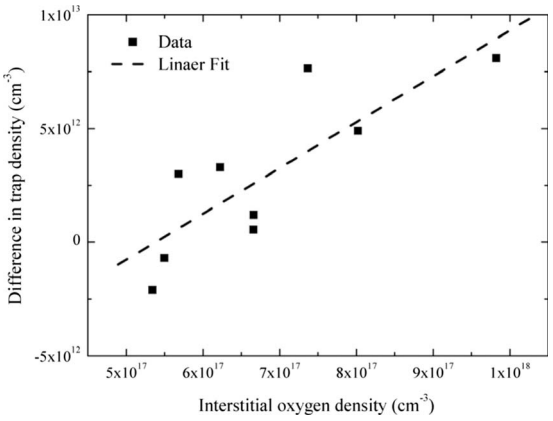

FIG. 8. Trap density in passivated Cz-specific defect state minus trap density in activated defect state against interstitial oxygen concentration. Linear fit points out the positive correlation.

nated. Parts of the ingots were annealed to ease the sawing of the wafers. The results of the trap density measurements are presented in Figs. 6 and 7. Figures 6 and 7 demonstrate that iron and molybdenum impurities can reduce the trap density. A comparable trend was observed in intentionally iron and intentionally titanium contaminated directionally solidified multicrystalline wafers. In Ref. 14 the concentration of dissolved iron and chromium in float zone wafers was shown not to be correlated with the trap density. Thus, the accumulation of metallic impurities at structural crystal defects could explain the existence of areas with high structural crystal defect densities and low trap densities in Figs. 4 and 5.

C. Trapping in Cz wafers

In boron doped Cz wafers a metastable defect was found,[15,16] which reduces the minority carrier lifetime in Cz wafers when it is in its activated state. This Cz-specific defect can be activated by illumination and passivated by a heat treatment.[15,16] The defect is attributed to boron-oxygen complexes BO_{2i}.[17] By the heat treatment the complexes are dissolved, and oxygen and boron are released. In Ref. 8 the effect of the Cz-specific defect on the trap density was examined and the trap density was found to be increased in the activated defect state compared to the passivated state. We examined a set of boron doped Cz samples from a standard ingot. The wafer surfaces are not passivated. Our results show that the difference between the trap density in the passivated defect state and the trap density in the activated defect state is positively correlated with the interstitial oxygen concentration and is in contradiction to Ref. 8, which is positive for high oxygen concentration. The difference in the trap density plotted against the interstitial oxygen concentration is depictured in Fig. 8. The examined wafers are standard boron doped and unpassivated Cz wafers. The interstitial oxygen concentration was determined by Fourier transform infrared (FTIR). The defect was activated by an illumination of 1000 W/m^2 for 14 h and passivated by annealing the wafers at 300 °C in the dark.

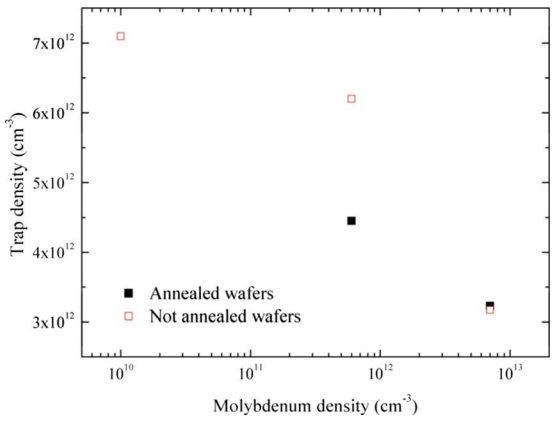

FIG. 7. (Color online) Trap density plotted against molybdenum density. As for iron, molybdenum shows the tendency to reduce the trap density.

We observed a decrease in the trap density with the activation of the Cz-specific defect in seven out of nine samples. This rules out an involvement of the Cz-specific effect in the formation of trap centers. The positive correlation between the difference in the trap density and the interstitial oxygen concentration on the other hand is an indication that oxygen plays an important role in trap centers, since oxygen is released from the BO_{2i} complexes by the heat treatment, and the Cz-specific defect density is positively correlated with the oxygen concentration.[18–20] Thus the amount of oxygen that is released during the annealing should be positively correlated with the interstitial oxygen concentration if boron is not the limiting component. Since also boron is released by the annealing, boron could also contribute to the trap density. This is checked in Fig. 9: the slightly negative trend of the difference against the boron concentration leads to the conclusion that oxygen is the dominant factor. This conclusion is supported by the fact that gallium doped Cz wafers show trap densities of the same magnitude as boron doped wafers.[8]

D. Effect of high temperature annealing on the trap density

The possible occurrence of thermal donors in Cz silicon is a well known fact (see, e.g., Ref. 21 for an overview). Thermal donors are formed during slow cooling between 300 and 600 °C and can be destroyed by an annealing step at 800 °C, whereas so-called "new thermal donors" (see, e.g.,

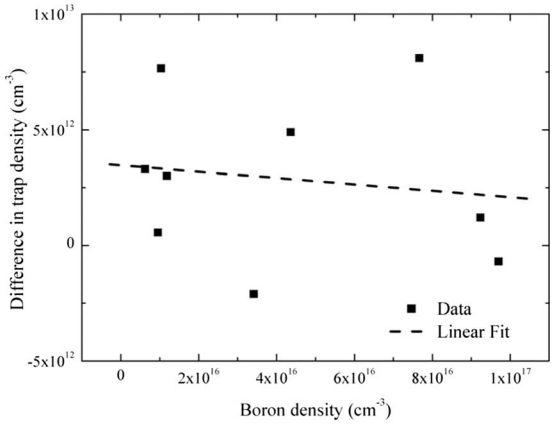

FIG. 9. Trap density in passivated Cz-specific defect state minus trap density in activated defect state against boron concentration. The linear fit illustrates that the difference does not significantly depend on the boron concentration.

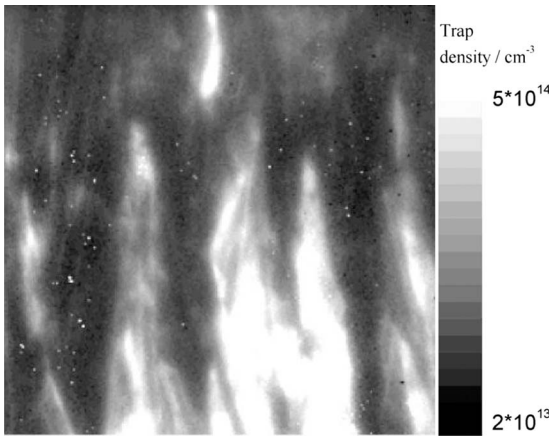

FIG. 10. Trap density image of a vertically cut as-cut wafer from the bottom region of a multicrystalline standard ingot. The bottom of the ingot is at the bottom of the image.

Ref. 20 for an overview) and oxygen precipitates are generated around 800 °C. New thermal donors differ from "old" thermal donors in their ionization energy, the maximum generation temperature, and the reaction to carbon.[21]

In Ref. 8 thermal donors were mentioned as a possible origin of trap centers. In order to scrutinize this hypothesis, the trap densities of 250 ± 5 μm thick as-cut Cz wafers from standard ingots with sufficiently high oxygen content were determined before and after an annealing step at 800 °C. The doping density before and after the annealing was measured by means of four point probe measurements. The doping density was increased by the annealing from 9.06×10^{14} cm^{-3} to a value close to the manufacturer specified doping density of 2.5×10^{15} cm^{-3}. The increase in the doping concentration indicates that thermal donors were destroyed during the annealing step. Since in parallel the trap density strongly increased from 1.06×10^{13} to 1.41×10^{14} cm^{-3}, thermal donors can be ruled out as the sole origin of trap centers. Therefore oxygen precipitates and new thermal donors arise as possible oxygen related origin of trap centers because both can be generated around 800 °C. This suggestion is also supported by the data in Ref. 22, which showed a positive correlation between doping density and trap density, and the observation in Ref. 23 that an increased doping density in turn enhances the formation of precipitates.

E. Relation between trap density and diffusion length in solar cells

In recent papers[4,24] a negative correlation between the trap density in as-cut wafers and the diffusion length in processed solar cells was reported for some examples. We studied the trap density across a multicrystalline ingot and found that the trap density itself, and also its correlation to the diffusion length, decreases from the bottom to the top of the ingot.

The trap density measured on a vertically cut wafer from the bottom region of a directionally solidified multicrystalline ingot with a doping concentration of 5.5×10^{15} cm^{-3} is shown in Fig. 10. In comparison, the image of the reciprocal lifetime of the solar cell processed on a neighboring wafer was calculated from a spectrally resolved light beam induced current (SR-LBIC) (Ref. 25) measurement and is depicted in Fig. 11.

The averaged decrease in trap density with height and the spatial correlation between trap density and diffusion length in this vertically cut wafer are presented in Figs. 12 and 13. Results showing the same trends were measured by CDI/ILM on other ingots. Interestingly, measurements done by quasi-steady-state photo conductance (QSSPC) in the literature[26] show different height dependent trap density profiles. This may be caused by differing impurity profiles in the respective crystals investigated or by the different measurement conditions: QSSPC measures under quasi-steady-state conditions whereas CDI/ILM measures under steady-state conditions, and trapping effects could thus be seen differently if traps are emptied slowly compared to typical minority carrier lifetimes.

Oxygen is the only known major impurity in silicon with a segregation coefficient greater than 1.[20] Therefore its concentration decreases from the bottom to the top of a multicrystalline block, which crystallizes from the bottom to the top. This behavior was confirmed by FTIR measurements of

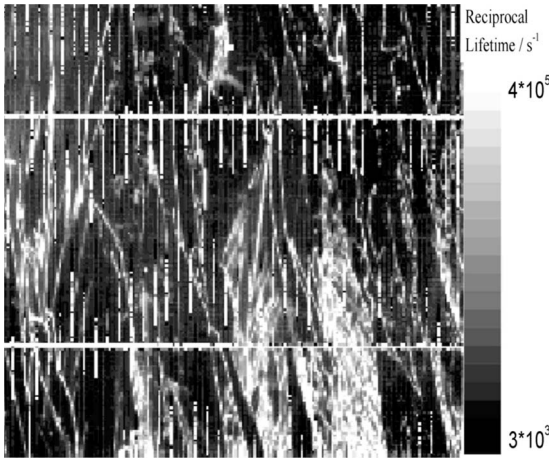

FIG. 11. Image of the reciprocal lifetime of the solar cell, which was processed from the wafer in Fig. 11. The reciprocal lifetime was calculated from SR-LBIC measurements.

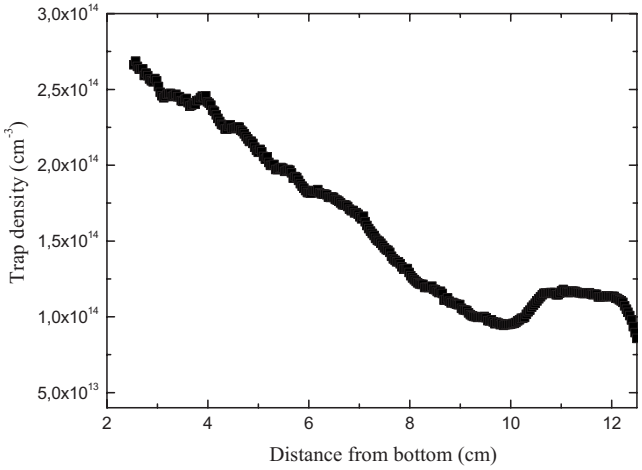

FIG. 12. Trap density against height. The trap density decreases with increasing distance from the bottom except for the topmost region.

the interstitial oxygen concentration $[O_i]$ on a wafer parallel to the investigated one in the Figs. 10–13: $[O_i]$ decreases from 6 ppm in 1 cm distance from the bottom to 3.5 ppm in 6 cm distance from the bottom, falling to values below the detection limit at greater height. Since oxygen correlated defects limit the diffusion length in the bottom region[27] and various impurities dominate in the top region,[28] the decrease in the trap density and its correlation to the diffusion length with height supports the notion that the traps in multicrystalline Cz silicon[8] are strongly correlated with oxygen related defects.

IV. CONCLUSIONS

We showed that structural crystal defects are necessary but not sufficient for the existence of high trap densities in some multicrystalline silicon samples. This could be due to the fact that structural crystal defects act as precipitation sites for impurities. Metallic impurities were demonstrated not to increase, rather decrease the trap density, and thus can be ruled out as a single origin of traps. Also the Cz-specific defect and thermal donors were shown not to be the main origin of trap centers. The comparison of the trap density in the activated Cz-specific defect state and the passivated state gave an indication that oxygen plays an important role in the formation of trap centers in Cz silicon. The increased trap density in Cz silicon after an 800 °C annealing gave rise to the suggestion that oxygen precipitates or new thermal donors, which can be generated at 800 °C, act as traps. The hypothesis that oxygen is at least partly responsible for the existence of traps was also supported by the height dependence in multicrystalline silicon ingots of the correlation between trap density in as-cut wafers and diffusion length in solar cells. Thus, the origin of increased trap densities in multicrystalline silicon could be structural crystal defects, which are highly decorated with oxygen precipitates.

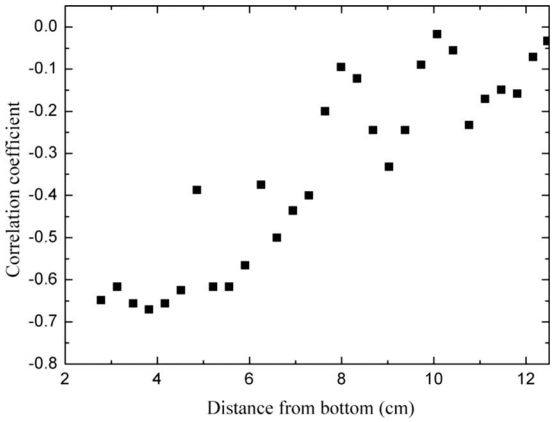

FIG. 13. Correlation coefficient between trap density in the as-cut wafer and diffusion length in the processed solar cell. The correlation is quite high in the bottom region and decreases with height.

ACKNOWLEDGMENTS

We would like to thank Holger Habenicht and Daniel Schwaderer for fruitful discussions, Tobias Kalden, Daniel Kray, Miroslawa Kwiatkowska, Harald Lautenschlager, and Antonio Leimenstoll for sample preparation, and Tonio Buonassisi for providing samples. We also thank the "CrystalClear" project funded by the European Commission under Contract No. SES6-CT_2003–502583 and especially Gianluca Coletti for providing some of the samples and the data on oxygen concentrations in the vertically cut wafers. These investigations were partly funded by the German Ministry for Research and Education under Contract No. 01SF0401.

[1] D. Macdonald and A. Cuevas, Appl. Phys. Lett. **74**, 1710 (1999).
[2] D. Macdonald and A. Cuevas, Sol. Energy Mater. Sol. Cells **65**, 509 (2001).
[3] P. Pohl, J. Schmidt, C. Schmiga, and R. Brendel, J. Appl. Phys. **101**, 073701 (2007).
[4] P. Gundel, M. C. Schubert, and W. Warta, Proceedings of the 22nd EU-PVSEC, Milan, Italy, 2007 (unpublished), pp. 1608–1612.
[5] H. Y. Fan, Phys. Rev. **92**, 1424 (1953).
[6] J. R. Haynes and J. A. Hornbeck, Phys. Rev. **100**, 606 (1955).
[7] M. C. Schubert, S. Riepe, S. Bermejo, and W. Warta, J. Appl. Phys. **99**, 114908 (2006).
[8] J. Schmidt, K. Bothe, and R. Hezel, Appl. Phys. Lett. **80**, 4395 (2002).
[9] P. Pohl, J. Schmidt, K. Bothe, and R. Brendel, Appl. Phys. Lett. **87**, 142104 (2005).
[10] M. C. Schubert, S. Riepe, and W. Warta, Proceedings of the 21st EU-PVSEC, Dresden, Germany, 2006 (unpublished), pp. 629–633.
[11] M. C. Schubert, S. Pingel, M. The, and W. Warta, J. Appl. Phys. **101**, 124907 (2007).
[12] T. F. Ciszek and T. H. Wang, J. Cryst. Growth **237–239**, 1685 (2002).
[13] G. Coletti, L. J. Geerligs, and P. Manshanden, Proceedings of the 22nd EU-PVSEC, Milan, Italy, 2007 (unpublished), pp. 989–993.
[14] D. H. Macdonald, Ph.D. thesis, The Australian National University, 2001.
[15] H. Fischer and W. Pschunder, Proceedings of the Idh. Eff. PVSC, Palo Alto, CA, 1973 (unpublished), pp. 404–411.
[16] J. Knobloch, S. W. Glunz, V. Henninger, W. Warta, W. Wettling, F. Schomann, W. Schmidt, A. Endrös, and K. A. Münzer, Proceedings of the 13th EU-PVSEC, Nice, France, 1995 (unpublished), pp. 9–12.
[17] J. Schmidt, K. Bothe, and R. Hezel, Proceedings of the 29th IEEE-PVSC, New Orleans, Louisiana, 2002 (unpublished), pp. 178–181.
[18] S. W. Glunz, S. Rein, W. Warta, J. Knobloch, and W. Wettling, Proceedings of the 2nd WC PVSEC, Vienna, Austria, 1998 (unpublished), pp. 1343–1346.
[19] J. Schmidt, A. G. Aberle, and R. Hezel, Proceedings of the 26th IEEE-PVSC, Anaheim, California, 1997 (unpublished), pp. 13–18.
[20] T. Yoshida and Y. Kitagawara, Proceedings of the 4th International Symposium on High Purity Silicon, San Antonio, Texas, 1996 (unpublished), pp. 450–454.
[21] A. Borghesi, B. Pivac, A. Sassella, and A. Stella, J. Appl. Phys. **77**, 4169 (1995).
[22] D. Macdonald, M. Kerr, and A. Cuevas, Appl. Phys. Lett. **75**, 1571 (1999).

[23]S. Matsumoto, I. Ishihara, H. Kaneko, H. Harada, and T. Abe, Appl. Phys. Lett. **46**, 957 (1985).
[24]M. C. Schubert and W. Warta, Prog. Photovoltaics **15**, 331 (2007).
[25]W. Warta, J. Sutter, B. F. Wagner, and R. Schindler, Proceedings of the Second WC PVSEC, Vienna, Austria, 1998 (unpublished), pp. 1650–1653.
[26]R. A. Sinton, T. Mankad, S. Bowden *et al.*, Proceedings of the 19th EU-PVSEC, Paris, France, 2004 (unpublished).
[27]D. Karg, Thesis, Universität Erlangen-Nürnberg, 1999.
[28]T. Buonassisi, A. A. Istratov, M. D. Pickett, M. Heuer, J. P. Kalejs, G. Hahn, M. A. Marcus, B. Lai, Z. Cai, S. M. Heald, T. F. Ciszek, R. F. Clark, D. W. Cunningham, A. M. G. R. Jonczyk, S. Narayanan, E. Sauar, and E. R. Weber, Prog. Photovoltaics **14**, 513 (2006).